

# DETERMINISTIC BEHAVIOR OF AN ANCHORING PLATE AND SENSITIVITY STUDY

M. LE NOIR DE CARLAN<sup>1,2</sup>, L. JASON<sup>1</sup> AND L. DAVENNE<sup>2</sup>

<sup>1</sup> Université Paris-Saclay, CEA, Service d'Etudes Mécaniques et Thermiques,  
91191 Gif-sur-Yvette, France.

<sup>2</sup> Laboratoire Energétique Mécanique Electromagnétisme (LEME), UPL, Université Paris Nanterre,  
92410 Ville d'Avray, France.

**Key words:** Damage, Anchorage, Finite Elements, Sensitivity Analysis

**Abstract:** The prediction of the resistance of concrete anchors is essential for ensuring the safety of sensitive infrastructures. This study proposes the use of an energetically regularized damage model in tension and compression (RTC), based on an extended version of Mazars' model. In addition to regularization, modifications have been made to better capture material behavior, particularly in compression, to simulate the pull-out tests of anchors. Finite element simulations using the Cast3M software are employed to analyze concrete cracking, considering both the behaviors of concrete and steel. The simulation results reveal two main failure modes: the formation of a concrete breakout cone or steel fracture. The first part of the study compares the results of experiments from the literature with simulations based on embedment length. The second part focuses on a sensitivity study of various parameters, including embedment length and plate stiffness. It appears that embedment length is a highly influential factor in the resistance of concrete anchors, and that anchor geometry can also have a significant impact.

## 1 INTRODUCTION

The design of anchors in reinforced concrete structures is a critical issue in sensitive installations. Current standards, particularly Eurocode 1992 Part 4 [1], assume that the anchor plate is infinitely rigid. It is therefore important to understand the impact of the plate's rigidity on the strength of a reinforced concrete structure, to evaluate the potential consequence of this assumption. Additionally, the influence of other parameters may also be worth investigating.

In the literature, different types of anchoring systems are observed, including cast-in-place [2] and post-installed anchors [3]. This study will focus on cast-in-place anchors with headed rods. This system has been chosen because it is commonly used in French nuclear power plants. The two main failure modes for this type of

anchors are bolt failure (steel failure) and concrete failure in the form of a cone [4 - 5].

A first part of the study focuses on the representation of pull-out and shear tests of a base plate. To verify the various aspects of the simulation, an initial simulation will model a simple stud test without a base plate. This simulation serves two purposes: first, to validate the constitutive relations in a simple case, and second, to evaluate the group effect of the studs on a base plate. Indeed, the group effect can reduce the resistance of a base plate by 30% in the test configurations [6].

The group effect in an anchorage refers to the reduction in the strength or individual efficiency of anchoring elements (such as studs or rods) when they are arranged in a group on the same base plate or in a similar attachment configuration. This effect results from the interactions between the stress zones generated

by each anchor [7].

Subsequently, pull-out and shear tests of a base plate with four studs will be simulated under these two loading conditions. The objective is to obtain reference tests and validate the steel and concrete models used, ultimately enabling sensitivity studies on certain parameters, such as the rigidity of the base plate and the embedment length ( $h_{ef}$ ).

To assess the impact of certain parameters on the strength, finite element simulations are conducted using the Cast3M software. A validation process is implemented for the steel and concrete models.

## 2 SIMULATION SPECIFICATION

The validation process is based on the experimental results from [8-9]. The objectives are to closely replicate the tests and verify that the failure modes and forces are accurately represented in the simulation. The simulations are performed using Cast3M software, version 2024 [10].

First, a pullout test for a single anchor bolt is modelled, considering different embedment lengths (Figure 1). This test was conducted in a  $2\text{m} \times 2\text{m} \times 0.6\text{m}$  concrete block with restraints at the ends (gray arrows).

This will ensure that the failure modes and maximum resistances correspond to the tests.

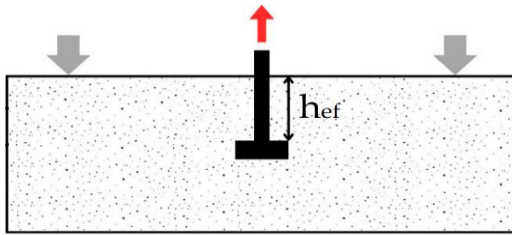


**Figure 1:** Diagram pullout test with single rod

Then, a complete anchoring system subjected will be modelled with two different loading conditions: pullout tests and shear tests. For each loading condition, various embedment lengths ( $h_{ef}$ ) will be tested (Figure 2).

Material parameters (Table 1) will remain constant throughout the validation phase.

**Table 1:** Material properties

	Young modulus (GPa)	Elastic limit (MPa)	Fracture energy (N/m)
Concrete tension	43	3	117
Concrete Compression	43	50	50000
Steel	210	365	

The simulations aims to closely replicate the experimental tests. To achieve this, the dimensions of the various elements (base plate, concrete block, and stud) are similar to those used in the experiments. The mechanical constraints of the tests will be represented by restricting the displacements in the blocked areas.

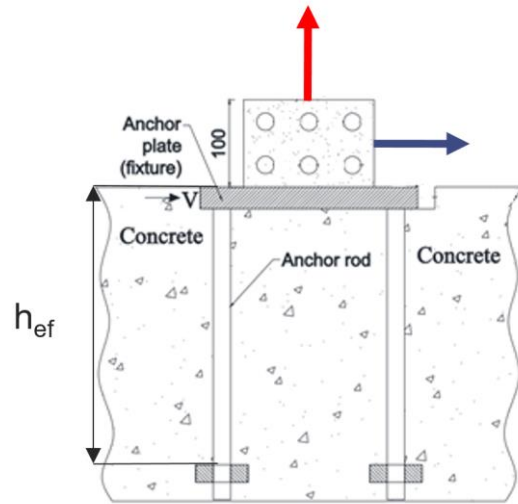


**Figure 2:** Diagram pullout and shear tests for a complete anchorage

The concrete mesh is as uniform as possible, with cubes of approximately 1 cm near the area of interest (close to the stud) (Figure 3). The steel meshes (anchor bolts and plate) will interact with the concrete through a frictionless sliding contact. The load will be applied through an imposed displacement on a portion of the base plate.

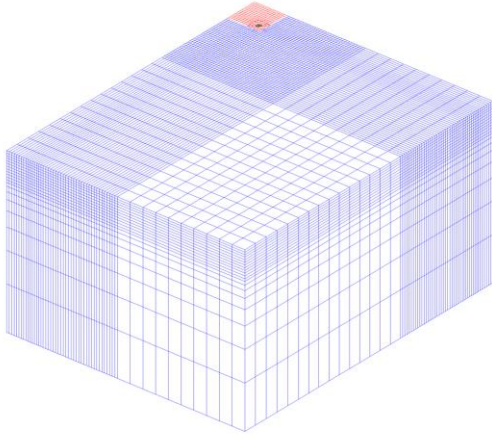


Figure 3: Mesh used for the simulation

## 2.1 Constitutive relations

The behavior models are described below. First, the steel behavior is based on the stress-strain curve available in the article [8], with a Von Mises criterion (Figure 4). The steel behavior curve was generated by extracting an experimental curve and reconstructing it from a table of values.

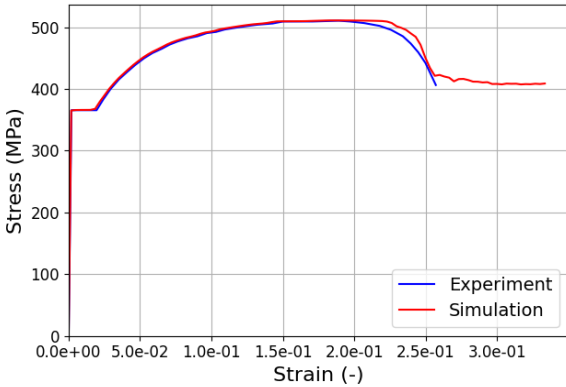


Figure 4: Comparison of simulation and experiment.

To better replicate the behavior of concrete and minimize the impact of meshing, a Mazars energy-regularized model for tension and compression was implemented. This model is based on a damage formulation (D). An energy-regularized model accounts for fracture energy, which corresponds to the area under the stress-displacement curve. Unlike the original version, this implementation introduces an

additional parameter  $G_{fc}$  to account for the softening slope in compression, improving the accuracy of post-peak behavior predictions.

The tensile behaviour (Figure 5) is governed by the tensile fracture energy  $G_{ft}$ .

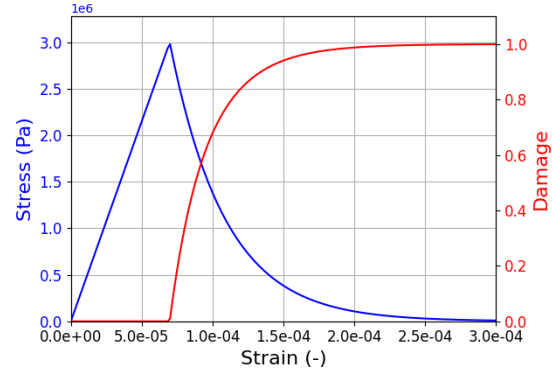


Figure 5: Constitutive law for concrete in tension

The compressive behavior is based on the FIB Code 2010, with the addition of a parameter  $G_{fc}$ , representing the fracture energy in compression. This parameter affects the softening slope (Figure 6). In the model, the softening part is represented by a straight line whose slope varies depending on  $G_{fc}$  and the element size. The other parameters representing the non-linearity of the behavior are described in reference [11].

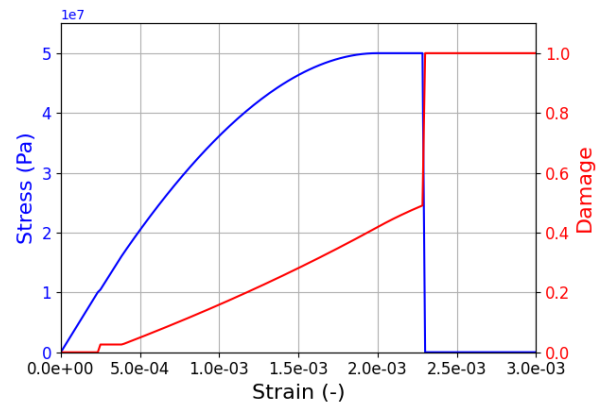


Figure 6: Constitutive law for concrete in compression

## 2.2 Simulations results

The results of the various pullout simulations with a single stud are presented below (Figure 7).

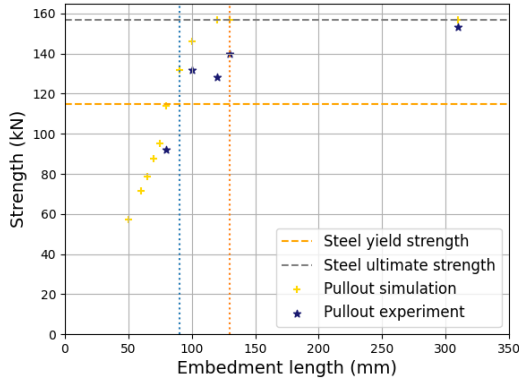


Figure 7: Single rod results

The simulation captures well the failure mode (concrete cone or steel failure). It is assumed that the concrete cracking cone is represented by the damage, which represents the loss of stiffness of the element.

Moreover, the magnitudes of the maximum resistances are consistent with expectations.

For an anchorage length between 50 and 90 mm, failure occurs in the form of a cone (Figure 8), and the stud remains in its elastic behavior. Between 90 and 130 mm, failure still occurs in the form of a cone, but the stud begins to yield. Beyond 130 mm, failure is due to the breaking of the stud.

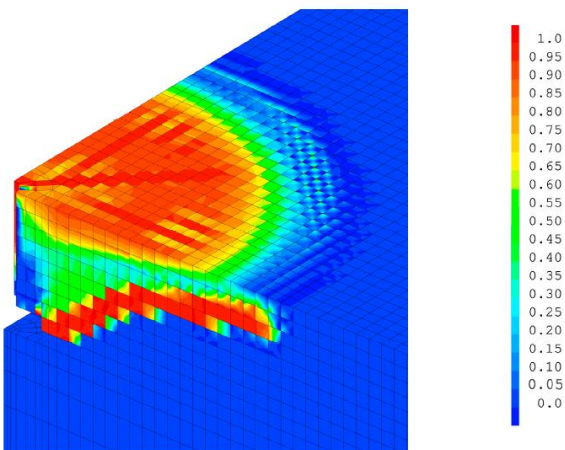


Figure 8: Damage distribution for an embedment length of 80 mm (single stud)

It is observed that the critical embedment length, representing the transition from concrete failure to steel failure, is approximately 100 mm. In this range, the results are highly sensitive and can vary

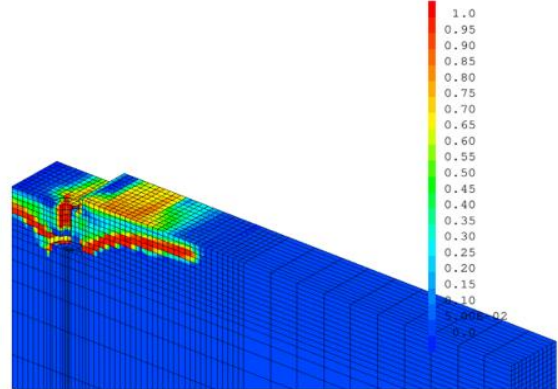


Figure 9: Damage distribution for a pullout test ( $h_{ef} = 80$  mm).

significantly with small changes in the embedment length. Indeed, for a difference of 1 cm in anchorage length, the resistance can increase by nearly 50 kN.

This initial study highlights the importance of embedment length on the results, as well as the accurate representation of failure modes using the reference numerical methodology.

The second study, focusing on the pullout of a complete anchoring system, yields the results shown below (Figure 10).

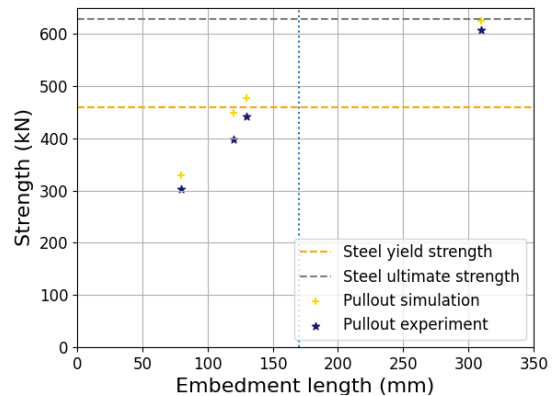


Figure 10: Pullout results of the complete anchoring system.

Similar to the first study, the failure modes are well represented. The simulation tends to underestimate the maximum force by approximately 10% in cases where concrete

failure occurs. For steel failure, the difference between the experimental results and the simulation is less than 1%.

Experimentally, under the test configuration, the group effect has an impact of around 30% [6].

On Figure 9, the concrete damage cone is observed extending to the right. The group effect is observed: the concrete damage propagates more horizontally in the direction of the other stud (not shown), whereas on the free side, the damage spreads in the form of a cone. This additional cracking reduces the effective strength of the surrounding material by causing stress interference between adjacent studs. This interaction limits the capacity of each stud to fully mobilize its resistance, leading to a collective reduction in the overall anchorage strength.

This magnitude is also observed in the simulations, demonstrating that the model accounts for the various interactions within the concrete.

Finally, the shear tests confirm the ability of the steel and concrete models to accurately represent another loading scenario (Figure 11).

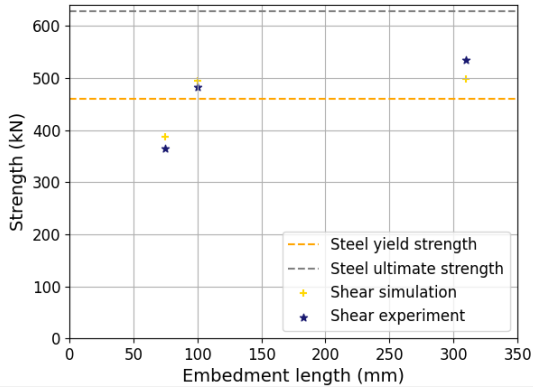


Figure 11: Shear results of the anchor

The approach has thus been successfully applied to various tests, accurately capturing the influence of anchor length and the emergence of different failure modes (such as concrete cone failure or steel rupture). Regardless of the applied loading conditions, the model consistently predicts the mechanical strength of the anchor. Furthermore, it

effectively simulates crack propagation in concrete while accounting for its failure mode. The simulations are therefore reliable enough to proceed with a sensitivity study.

### 3 SENSITIVITY STUDY

The sensitivity study is based on a pullout simulation of a complete anchoring system. The parameters of the study allow for two symmetries, enabling the simulation of only one-quarter of the experiment. The initial material and geometric parameters for the simulation are based on those described in [12].

Using the validated modeling strategy outlined in the previous section, a preliminary sensitivity study was conducted on three parameters: the embedment length, the load application surface (red zone Figure 12), and the Young's modulus of the anchor plate.

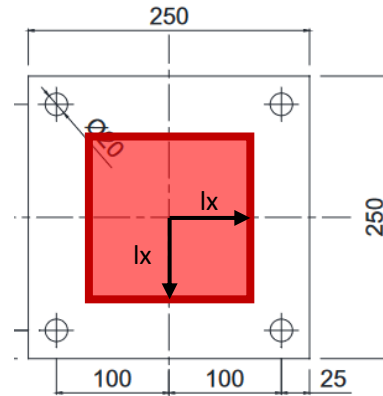


Figure 12: Representation of the loading surface on the base plate

These parameters were selected for two reasons: their simplicity in terms of simulation modeling, and their potential to confirm or refute trends observed during the model validation.

$$F(x_{i,j}) = b_0 + \sum_{i=1}^k b_i x_i + \sum_{i=1}^k \sum_{j=i}^k b_{ij} x_i x_j \quad (1)$$

This sensitivity study relies on the response surface methodology, assuming a second-degree polynomial interpolation ( 1 ) to describe the evolution of anchor strength as a function of the input parameters.

The experimental design is constructed using a matrix with values of 1, 0, and -1. For each parameter, 1 represents the maximum value, -1 the minimum value, and 0 the average value. With three parameters to vary, there are a total of 12 configurations.

**Table 2** : Design matrix

Config	x1	x2	x3
1	1	1	0
2	-1	1	0
3	1	-1	0
4	-1	-1	0
5	1	0	1
6	-1	0	1
7	1	0	-1
8	-1	0	-1
9	0	1	1
10	0	1	-1
11	0	-1	1
12	0	-1	-1

This experimental design (Table 2) can be visualized in a three-dimensional space (Figure 13). The red points represent the different configurations, with each configuration positioned equidistant from the center. This ensures that each simulation holds equal importance in the analysis.

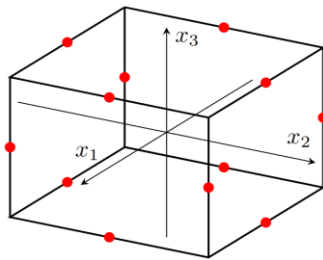


**Figure 13**: Experimental design in 3D space

In this initial study, the embedment length ( $h_{ef}$ ) varies from 8 cm to 15 cm, the load application area ( $l_x$ ) from 1 cm to 10 cm, and the Young's modulus ( $E$ ) of the plate from 20 GPa to 2000 GPa. These variation ranges were selected to capture the bending of the plate while ensuring that the failure mode remains concrete failure.

Starting with the construction matrix (Table 2) for three variables, the experimental design consists of 12 simulations (Table 3). The output variable will be the maximum force,  $F_{max}$ .

**Table 3**: Experimental matrix

Config	$h_{ef}$	$l_x$	$E$
1	0,15	0,1	1,01E+12
2	0,08	0,1	1,01E+12
3	0,15	0,01	1,01E+12
4	0,08	0,01	1,01E+12
5	0,15	0,055	2E+12
6	0,08	0,055	2E+12
7	0,15	0,055	2E+10
8	0,08	0,055	2E+10
9	0,115	0,1	2E+12
10	0,115	0,1	2E+10
11	0,115	0,01	2E+12
12	0,115	0,01	2E+10

From these 12 simulations, an interpolated surface is obtained using the least squares method, fitting as closely as possible to the calculated points. The response surfaces in the space ( $h_{ef}$ ,  $l_x$ ,  $F_{max}$ ) for three different plate stiffness values are shown (Figure 14).

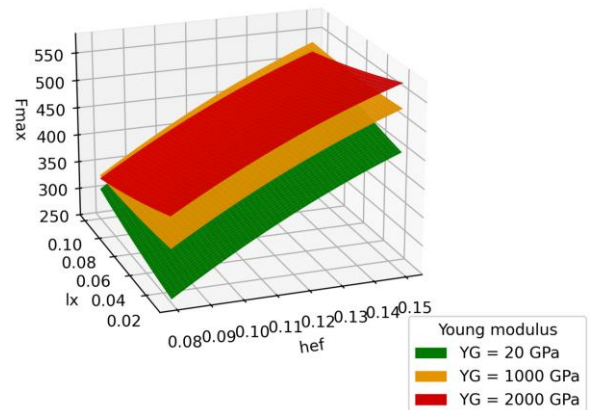


**Figure 14**: Interpolated surface

A general trend emerges: the greater the embedment length, the higher the maximum force. This trend was already observed in the validation section (2). In the case of a soft plate, the impact of the loading area is present; for a

large loading area, the maximum resistance is higher than for a small loading area. This trend holds true regardless of the embedment length. For a stiffer plate, the impact of the loading area is more limited. The maximum force depends on the plate's bending. The more the plate bends, the weaker the anchorage resistance becomes. The plate bends if the loading area is small or if the Young's modulus is low.

This first study confirms the trends observed in the unitary calculations, as well as the significant impact of the plate's rigidity. It represents the first step toward a more in-depth analysis that will allow for a more precise quantification of these effects.

#### 4 CONCLUSION

The first part of this document demonstrates that the steel and concrete models accurately reproduce the various pull-out and shear experiments. It is followed by a parametric study that confirms the observed trends, particularly regarding the impact of anchor length, and demonstrates the ability of the response surface method to quantify the influence of key factors.

The future work will focus on continuing sensitivity analyses. A comparison between the response surface method and a parametric study with a more traditional design of experiment will also be carried out. The inclusion of new parameters will be considered, such as the eccentricity and angle of loading, the diameter of the rod, and the head of the stud. The aim of these results is to identify the most influential parameters and quantify their impact on the mechanical system's strength.

#### REFERENCES

[1] AFNOR, NF EN 1992-4 — Design of concrete structures — Part 4: design of fastenings for use in concrete. 2018.  
 [2] Q. T. Bao, K. Lee, H. An, D. H. Lee, et J. Shin, Effective prediction finite element model of pull-out capacity for cast-in-place anchor in high strain rate effects, Sci

Rep, vol. 13, n° 1, p. 18070, oct. 2023, doi: 10.1038/s41598-023-44510-y.  
 [3] H. Alhaidary et A. K. Al-Tamimi, Importance of performance certification for post-installed anchors: An experimental assessment, Structures, vol. 29, p. 273-285, févr. 2021, doi: 10.1016/j.istruc.2020.11.005.  
 [4] R. Ballarini, S. P. Shah, L. M. Keer, et I. N. Sneddon, Failure characteristics of short anchor bolts embedded in a brittle material, Proceedings of the Royal Society of London. A. Mathematical and Physical Sciences, vol. 404, n° 1826, p. 35-54, janv. 1997, doi: 10.1098/rspa.1986.0017.  
 [5] R. Eligehausen et G. Sawade, A fracture mechanics based description of the pull-out behavior of headed studs embedded in concrete, janv. 1989, doi: 10.18419/opus-7930.  
 [6] M. Węglorz, Influence of Headed Anchor Group Layout on Concrete Failure in Tension, Procedia Engineering, vol. 193, p. 242-249, 2017, doi: 10.1016/j.proeng.2017.06.210.  
 [7] J. Ožbolt, R. Eligehausen, et H. W. Reinhardt, Size effect on the concrete cone pull-out load, in Fracture Scaling, Z. P. Bažant et Y. D. S. Rajapakse, Éd., Dordrecht: Springer Netherlands, 1999, p. 391-404. doi: 10.1007/978-94-011-4659-3\_22.  
 [8] T. T. Bui, A. Limam, W. S. A. Nana, B. Arrieta, et T. Roure, Cast-in-place Headed Anchor Groups Under Shear: Experimental and Numerical Modelling, Structures, vol. 14, p. 178-196, juin 2018, doi: 10.1016/j.istruc.2018.03.008.  
 [9] F. Delhomme, T. Roure, B. Arrieta, et A. Limam, Pullout behavior of cast-in-place headed and bonded anchors with different embedment depths, Mater Struct, vol. 49, n° 5, p. 1843-1859, mai 2016, doi: 10.1617/s11527-015-0616-4.  
 [10] CEA, Cast3M. [Online]. Available on: <https://www-cast3m.cea.fr/>  
 [11] M. R. T. Arruda, J. Pacheco, L. M. S. Castro, et E. Julio, A modified Mazars damage model with energy regularization, Engineering Fracture Mechanics, vol. 259,

p. 108129, janv. 2022, doi:  
10.1016/j.engfracmech.2021.108129.

- [12] G. E. P. Box et D. W. Behnken, Some  
New Three Level Designs for the Study of  
Quantitative Variables, *Technometrics*,  
vol. 2, n° 4, p. 455-475, 1960, doi:  
10.2307/1266454.